

Perceive-Sample-Compress: Towards Real-Time 3D Gaussian Splatting

Zijian Wang ^{*} ¹, Beizhen Zhao ^{*} ¹, Hao Wang [†] ¹

¹ The Hong Kong University of Science and Technology (Guangzhou)
zwang886@connect.hkust-gz.edu.cn, bzhao610@connect.hkust-gz.edu.cn, haowang@hkust-gz.edu.cn

Abstract

Recent advances in 3D Gaussian Splatting (3DGS) have demonstrated remarkable capabilities in real-time and photorealistic novel view synthesis. However, traditional 3DGS representations often struggle with large-scale scene management and efficient storage, particularly when dealing with complex environments or limited computational resources. To address these limitations, we introduce a novel perceive-sample-compress framework for 3D Gaussian Splatting. Specifically, we propose a scene perception compensation algorithm that intelligently refines Gaussian parameters at each level. This algorithm intelligently prioritizes visual importance for higher fidelity rendering in critical areas, while optimizing resource usage and improving overall visible quality. Furthermore, we propose a pyramid sampling representation to manage Gaussian primitives across hierarchical levels. Finally, to facilitate efficient storage of proposed hierarchical pyramid representations, we develop a Generalized Gaussian Mixed model compression algorithm to achieve significant compression ratios without sacrificing visual fidelity. The extensive experiments demonstrate that our method significantly improves memory efficiency and high visual quality while maintaining real-time rendering speed.

Introduction

3D Gaussian Splatting (3DGS) (Kerbl et al. 2023) has revolutionized the field of novel view synthesis (NVS) (Avidan and Shashua 1997; Watson et al. 2022; Choi et al. 2019; Riegler and Koltun 2020; Dalal et al. 2024), offering a compelling solution to traditional volumetric rendering and mesh-based methods (Yariv et al. 2023; Lombardi et al. 2019; Penner and Zhang 2017; Wizaradwongsa et al. 2021; Zhou et al. 2018). By representing scenes as a set of anisotropic Gaussians, 3DGS achieves remarkable photorealism and real-time rendering speeds, quickly becoming a cornerstone technology for 3D reconstruction.

Despite its impressive capabilities, a key challenge lies in managing the computational complexity and storage requirements when scenes involve millions of Gaussian points. The direct application of 3DGS to large-scale or memory-constrained scenarios lacks efficient management representation (Wang and Xu 2024; Liu et al. 2024b; Chen

et al. 2024a), resulting in inconsistencies and degradation when rendering scenes at different scales. When scenes involve millions of Gaussian primitives, the dense collection of Gaussians can lead to excessive memory consumption and computational demands, hindering its scalability.

Existing methods struggle to effectively address the challenges of storage consumption and hierarchical scalability simultaneously. Some attempts to address the storage consumption of Gaussian Splatting, such as Scaffold-GS (Lu et al. 2024), HAC++ (Chen et al. 2025) and Context-GS (Wang et al. 2024), lack explicit Level-of-Detail (LOD) (David et al. 2003) mechanisms. This absence results in inefficient storage and rendering, as the entire scene representation must be processed regardless of the viewer’s proximity or the required level of detail. Other approaches, like Octree-GS (Ren et al. 2024), while introducing hierarchical structures, can be overly dependent on camera distance to optimize the whole structure and may lead to sub-optimal performance in scenes with complex geometric distributions, as they might over-prune crucial details and fail to capture fine-grained information.

To overcome these limitations, we introduce a novel perceive-sample-compress framework for 3D Gaussian Splatting. We propose a scene perception compensation algorithm that refines the parameters at each level. Unlike existing methods that rely solely on camera distance, our algorithm dynamically prioritizes optimization efforts based on camera coverage area and depth of field. This algorithm intelligently prioritizes visual importance for higher fidelity rendering in critical areas, while optimizing resource usage and improving overall visible quality.

Then, based on the levels of perception areas, we propose a pyramid sampling representation inspired by the Laplacian pyramid and voxelization. This approach allows us to group and represent Gaussians at multiple scales for each level of the pyramid. By voxelizing the scene and applying pyramid to aggregate Gaussian properties within these voxels, we establish a hierarchical multi-scale scene structure. This pyramid representation significantly enhances memory efficiency and enables adaptive rendering strategies.

Finally, we propose a generalized Gaussian mixed model compression algorithm based on the hierarchical pyramid structure. By analyzing the distribution of Gaussian attributes across hierarchical levels, we can effectively encode

^{*}These authors contributed equally to this work.

[†]Corresponding author.

redundant information and reduce the model size, making our framework more practical for storage and transmission.

In summary, our work makes three key contributions:

- We introduce a scene perception compensation algorithm that intelligently refines Gaussian parameters at each level based on camera coverage area and depth of field, leading to improved visual quality.
- We propose a pyramid sampling function for 3D Gaussian Splatting by combining Laplacian pyramid with voxelization, enabling efficient hierarchical representation and adaptive processing of large-scale scenes.
- We develop a compression algorithm based on generalized Gaussian distribution for efficient storage of our Gaussian representations, significantly reducing memory consumption and facilitating broader applicability.

Related Work

Level-of-Detail 3DGS

Level-of-Detail (LOD) (David et al. 2003) is a classic and critical technique in computer graphics that effectively manages the rendering budget of 3D scenes to improve rendering efficiency. Several works have explored LOD mechanisms in Gaussian-based scene representations (Cui et al. 2024; Seo et al. 2024; Milef et al. 2025; Ren et al. 2024; Wang and Xu 2024; Liu et al. 2024b; Kerbl et al. 2024). For example, LetsGo (Cui et al. 2024) employs a multi-resolution Gaussian model and jointly optimizes multiple levels. However, the rendering quality is highly dependent on multi-resolution point cloud inputs, which significantly increases training overhead. CityGaussian (Liu et al. 2024b) improves efficiency of large-scale scenes by selecting and blending LOD levels based on distance intervals, but requires manual setting of distance thresholds, which results in a lack of robustness. While Octree-GS (Ren et al. 2024) significantly improves rendering speed through its use of an explicit octree structure and a cumulative LOD strategy, its level selection strategy relies excessively on camera distance, making it prone to losing critical visual details due to improper level switching in complex and heavily occluded scenes.

Compression of 3DGS

Although 3DGS (Kerbl et al. 2023) demonstrates outstanding performance in terms of rendering speed and image fidelity, the large number of Gaussians and their associated parameters result in significant storage overhead. To address this issue, researchers have proposed various compression strategies. (Lee et al. 2024; Niedermayr, Stumpfegger, and Westermann 2024; Girish, Gupta, and Shrivastava 2024; Fan et al. 2024; Navaneet et al. 2023; Papantonakis et al. 2024; Ali et al. 2024; Wang et al. 2024; Liu et al. 2024a; Chen et al. 2024b, 2025) For example, the work in (Niedermayr, Stumpfegger, and Westermann 2024; Navaneet et al. 2023) introduces codebooks to cluster Gaussian parameters, while the studies in (Papantonakis et al. 2024; Ali et al. 2024) systematically explore pruning-based optimization methods. Building on Scaffold-GS (Lu et al. 2024), Context-GS (Wang et al. 2024) and CompGS (Liu et al.

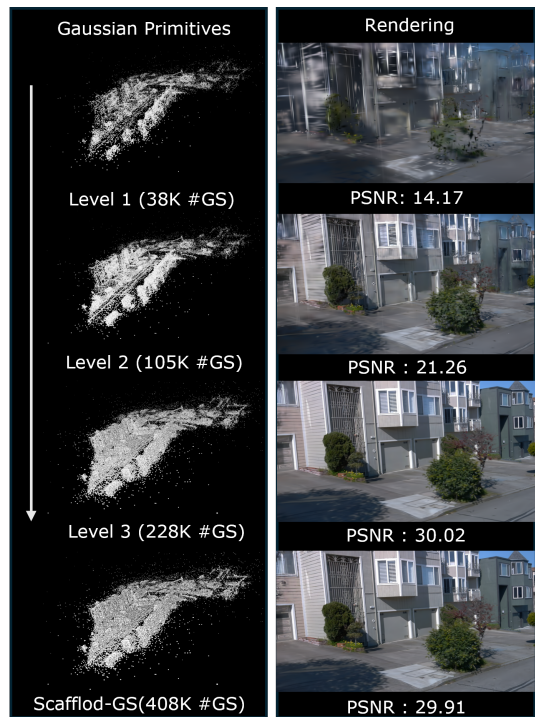


Figure 1: **Visualization of pyramid level** Compared with Scaffold-GS, our method can achieve higher PSNR scores with fewer Gaussian primitives.

2024a) adopt context-aware approaches that explicitly incorporate hierarchical relationships among anchors and Gaussians to enhance representational capacity. HAC++ (Chen et al. 2025) further introduces hashed features as priors for entropy coding and demonstrates its effectiveness in improving compression efficiency. However, these methods heavily rely on the anchor selection mechanism proposed in Scaffold-GS, and fail to fully model the distributional differences among various Gaussian parameters during encoding stage.

Methodology

Our proposed approach aims to address the limitations of traditional 3DGS by introducing a robust pyramid structure framework. This framework is built upon three interconnected components: a scene perception compensation algorithm that leverages camera coverage and depth of field for improved rendering quality, a hierarchical pyramid sampling representation with voxelization for efficient scene management, and a compression scheme for effective model storage. These components interact seamlessly, with the pyramid sampling establishing the foundation for multi-scale detail, the camera-driven compensation refining pyramid level partition accuracy, and the compression scheme ensuring scalability for large scenes. The overall goal is to create a scalable, efficient, and high-fidelity 3D representation. This section details the technical implementation of these components. The overall pipeline is shown in Fig. 2.

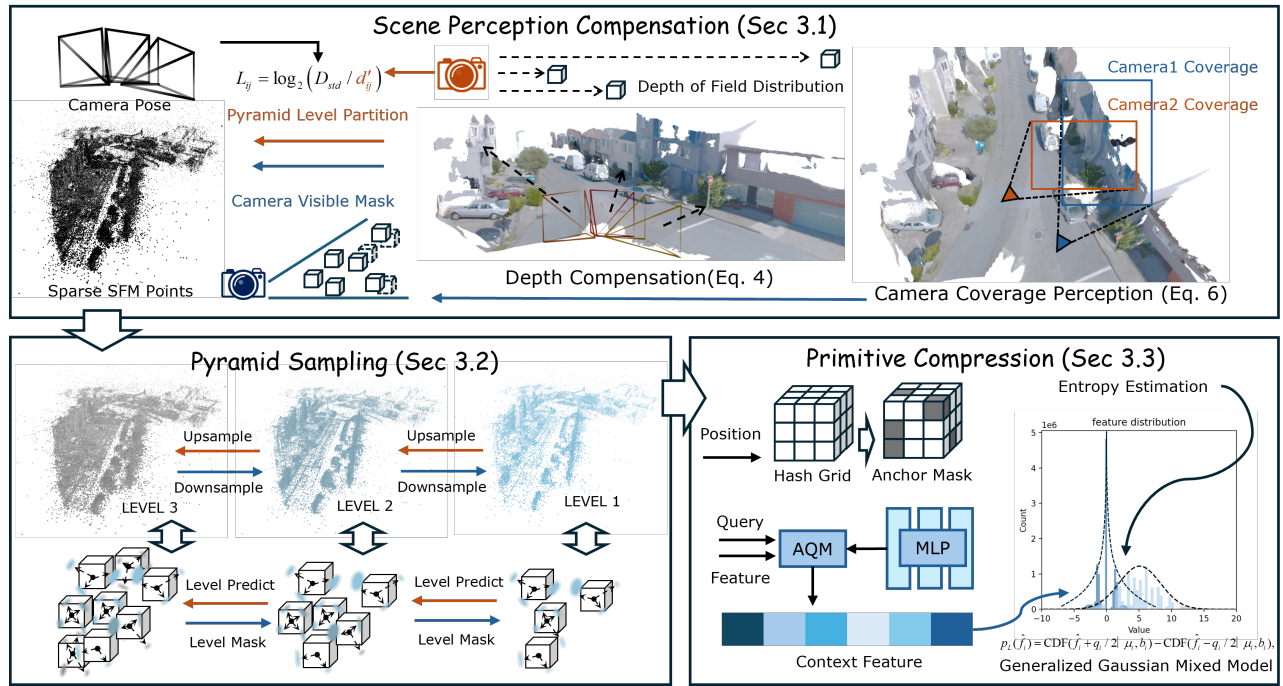


Figure 2: **Framework of Pyramid-GS.** We begin by sampling the input sparse point cloud. We propose a scene perception compensation algorithm, which take the camera coverage and depth of field accounts for pyramid level partition. Then we design a hierarchical pyramid sampling representation to set up pyramid structure. Finally, we utilize compression algorithm for efficient storage while maintaining real-time rendering speed and photorealistic visual effects. An adaptive quantization module (AQM) is used to generate context feature, while the generalized gaussian mixed model is used for entropy estimation.

Scene Perception Compensation

To refine the pyramid level partition and ensure perceptual quality, we introduce a compensation algorithm that considers camera coverage and depth of field (DOF) effects. Our algorithm aims to dynamically adjust the perceived importance of anchors based on their visibility and how they are affected by the camera’s optical properties. We model this by computing a visibility score for each anchor, which incorporating both camera coverage and depth perception.

We approximate the DOF effect by analyzing the distribution of points along the principal viewing direction from the camera. For a set of anchors $\{A_k\}$ with position $\mathbf{p}_k \in \mathbb{R}^3$, we can estimate the variance of their projected distances from the camera. Let $\mathbf{d}_k = \mathbf{p}_k - \mathbf{c}_j$ be the vector from the camera to the k -th anchor. We identify the main axis of dispersion \mathbf{m}_j for these points. The projected depth for A_k is $z_k = |\mathbf{d}_k \cdot \mathbf{m}_j|$. We then compute the standard deviation of these projected depths, where $\sigma_{z,j} = \text{std}(z_k)$.

A large $\sigma_{z,j}$ indicates that many points are spread out in depth, suggesting a shallow DOF or a scene with significant depth variation. In such cases, we apply a depth compensation factor f_{depth} to the distance used for pyramid level partition. This factor is designed such that a larger $\sigma_{z,j}$ leads to a smaller f_{depth} , effectively making objects appear ”closer” in terms of pyramid priority, thus encouraging their representation at finer levels. The formulation is as follows:

$$f_{depth} = 1 + \alpha \cdot \max(0, \frac{\sigma_{z,j}}{\sigma_{z,thresh}} - 1), \quad (1)$$

where α is a superparameter and $\sigma_{z,thresh}$ is a threshold for DOF significance. The adjusted distance d'_{ij} for pyramid level partition for anchor A_i from camera c_j becomes $d'_{ij} = d_{ij} \cdot f_{depth}$, where $d_{ij} = \|\mathbf{p}_i - \mathbf{c}_j\|$. The pyramid level L_{ij} for A_i from camera c_j is then determined based on this adjusted distance, typically using a logarithmic scale:

$$L_{ij} = \log_2 \left(\frac{D_{std}}{d'_{ij}} \right), \quad (2)$$

where D_{std} is a standard reference distance. This value is then mapped to an integer pyramid level.

For each camera c_j with center \mathbf{c}_j and intrinsic parameters, we first determine the visible anchors. An anchor is considered visible to camera c_j if its predicted pyramid level L_{ij} is smaller or equal to the current level. We then count the number of cameras $N_{vis,i}$ that render at least one anchor at current level. The normalized coverage score for G_i is

$$C_i = \beta \frac{N_{vis,i}}{N}. \quad (3)$$

Then we calculate the mean value of the counts of visible anchors for each camera as the visible threshold τ . The final visible threshold is updated through the coverage score C . We can utilize this threshold for camera visibility control through a mask for scene perception.

$$\tau_{new} = (1 + C)\tau_{old}. \quad (4)$$

This scheme ensures that points with larger depth variation, often corresponding to distant or complex regions, are allocated appropriate levels to maintain visual quality. The method enhances the initialization and refinement of pyramid levels, leading to more accurate scene representations.

Pyramid Sampling Representation

To enable efficient management of Gaussian primitives, we introduce a hierarchical representation inspired by Laplacian pyramid and voxelization. Traditional methods often lack explicit level control, leading to uniform processing of all Gaussians, which is inefficient for large scenes. Our approach tackles this by organizing Gaussians into a multi-scale structure. To effectively represent the scene at multiple levels of detail, we employ a Laplacian pyramid framework that decomposes the scene into several resolution layers. At each level, scene features are captured with varying degrees of detail, enabling scalable rendering and processing.

Given an input point cloud $\mathcal{P} = \{p_i \in \mathbb{R}^3\}_{i=1}^N$, we construct a Laplacian pyramid with L levels through iterative voxelization. First, we recursively group voxels into smaller blocks. At each level of the pyramid, Gaussians within a block are voxelized into representative anchors. This aggregation is performed using principles akin to the Laplacian pyramid construction, where each level captures the high-frequency details relative to the coarser level below:

$$\mathcal{V}'_{l-1} = \mathcal{R}_{l-1} \cap \mathcal{P}, \quad \mathcal{R}_{l-1} = \text{Downsample}(\mathcal{V}'_l, \rho_{l-1}), \quad (5)$$

where \mathcal{V}_l denotes the voxelized points at level l with resolution $\rho_l = 2^{-l}\rho_0$, and \mathcal{R}_l stores residuals. Through the downsample process, we get a simple multi-scale structure representation. Then we execute an upsample process to sample detail residuals of each level.

$$\mathcal{V}_l = \mathcal{R}_l \cup \mathcal{V}'_l, \quad \mathcal{R}_l = \text{Upsample}(\mathcal{V}'_{l-1}, \rho_l). \quad (6)$$

The core idea is to maintain a set of Gaussians that are adaptively represented across different spatial resolutions. The coarsest level represents the overall scene structure, while finer levels provide increasing detail. This allows us to selectively process parts of the scene at an appropriate resolution based on the viewing context. This voxel-based, pyramidal representation significantly reduces the number of active Gaussians and improves memory efficiency compared to a flat representation. After voxelizing \mathcal{P} into a grid \mathcal{V} , each voxel is parameterized by Gaussian functions predicted through a multi-layer perceptron (MLP):

$$\mathcal{G}_l(\mathbf{x}) = \{F^\sigma(\mathbf{x}_l), F^\mu(\mathbf{x}_l), F^\alpha(\mathbf{x}_l), F^c(\mathbf{x}_l)\}, \quad (7)$$

where \mathcal{G}_l denotes the Gaussian representation at level l . F^σ , F^μ , F^α and F^c represent the MLP network to generate variance σ_l , mean μ_l , opacity α and color c of the gaussians.

This multi-scale decomposition allows us to represent scene details hierarchically, such that coarse layers capture the global structure and finer layers preserve details—enabling efficient rendering and bias towards important scene features at different pyramid levels.

Generalized Gaussian Mixed Compression

To ensure the scalability of Pyramid-GS, we propose an efficient model compression strategy based on context-aware entropy coding, targeting anchor features across pyramid levels. Drawing inspiration from HAC++ (Chen et al. 2025), which employs hash-grid features to assist an Adaptive Quantization Module (AQM) for Gaussian parameter prediction, we introduce a key modification to the probability model to better capture the statistical characteristics of our hierarchical representation.

In image and video compression, the Generalized Gaussian Distribution (GGD) effectively models transform or prediction residuals. We adopt GGD to uniformly characterize diverse parameter distributions in our framework. Notably, high-frequency components in the pyramid exhibit sparsity, with distributions sharply peaked at zero and heavy tails, aligning with the Laplace distribution (GGD with $\beta = 1$). In contrast, other parameters resemble Gaussian distributions (GGD with $\beta = 2$), as illustrated in Fig. 2. GGD offers a statistically sound foundation, enabling the application of tailored priors to different parameters within the framework. Its probability density function (PDF) is defined as:

$$p(x|\mu, \alpha, \beta) = \frac{\beta}{2\alpha\Gamma(1/\beta)} \exp\left(-\left(\frac{|x-\mu|}{\alpha}\right)^\beta\right), \quad (8)$$

where μ is the location parameter, α is the scale parameter, and β is the shape parameter that controls the distribution’s tail behavior. Following HAC++ (Chen et al. 2025), we use a lightweight MLP, denoted as MLPc, to predict the probability distribution parameters for a given Gaussian attribute \hat{f}^i from its spatial hash-grid feature f_h^i . Our MLPc estimates the location μ_i and scale α_i parameters for the distribution. The shape parameter β_i , however, is pre-set according to the type of parameter being compressed: for high-frequency residual features, we set $\beta_i = 1$ (Laplace), while for other parameters, we set $\beta_i = 2$ (Gaussian).

The probability of the quantized attribute \hat{f}^i with a quantization step q_i is then calculated by integrating the corresponding GGD’s PDF over the quantization bin:

$$p_{\text{GGD}}(\hat{f}^i) = \text{CDF}(\hat{f}^i + q_i/2 | \mu_i, \alpha_i, \beta_i) - \text{CDF}(\hat{f}^i - q_i/2 | \mu_i, \alpha_i, \beta_i), \quad (9)$$

where $\text{CDF}(x|\mu, \alpha, \beta)$ is the cumulative distribution function of the GGD, with $\mu_i, \alpha_i = \text{MLPc}(f_h^i)$ and β_i being the pre-set value. This design allows the model to leverage the generality of the GGD framework to impose the most fitting inductive bias on data with different statistical characteristics, thereby maximizing compression efficiency.

This compression module is applied to the attributes of Gaussians at each level of our pyramid. The entire model is trained end-to-end by minimizing a rate-distortion loss, which balances rendering quality and model size:

$$\mathcal{L} = \mathcal{L}_{\text{render}} + \lambda \left(\frac{1}{N} \sum_{i=1}^N -\log_2 p_{\text{GGD}}(\hat{f}^i) + \mathcal{L}_{\text{hash}} \right). \quad (10)$$

Here, $\mathcal{L}_{\text{render}}$ combines fidelity losses akin to Scaffold-GS, while the second term denotes the overall rate loss, comprising the average entropy of primitive attributes and the

hash-grid entropy. With N as the number of primitives and λ controlling the quality–compression trade-off, this formulation encourages compact yet high-fidelity representations.

Experiment

In this section, we begin by outlining the datasets used for our evaluation and providing the specific implementation details of our experiments. Then we present our main comparison results and the ablation study and related discussions.

Dataset

To evaluate the performance and scalability of our model, we selected 17 scenes from four widely-used datasets.

Small-Scale Datasets. To evaluate rendering fidelity on complex, object-centric scenes, we use two standard datasets. Mip-NeRF 360 (Barron et al. 2022) contains seven challenging scenes featuring unbounded 360° camera trajectories, with approximately 200 images per scene. Tanks & Temples (Knapitsch et al. 2017) is used for assessing the reconstruction of fine-grained geometric details, each scene containing over 200 images.

Large-Scale Datasets. To demonstrate the scalability in large-scale environments, we employ two distinct datasets. Waymo Open Dataset (Sun et al. 2020) provides real-world autonomous driving scenarios. We utilize six sequences, each with around 600 frames, to test our model’s ability to handle extensive environments and long camera paths. Matrix City (Li et al. 2023) is a massive, city-scale dataset that tests the limits of scalability. Following Octree-GS (Ren et al. 2024), we test on a blocksmall partition which showcases the effectiveness of our hierarchical framework in extremely large-scale reconstruction and rendering tasks.

Implementation Details

We implemented our Pyramid-GS framework in PyTorch. All experiments were conducted on a single NVIDIA RTX A6000 GPU with CUDA 11.6, and models were trained for 40,000 iterations using the Adam optimizer. For our Pyramid sampling, the number of levels L is automatically set according to the dataset. Regarding the Scene Perception Compensation module, the depth of field standard threshold $\sigma_{z, \text{thresh}}$ is set to 50.0, with a corresponding distance compensation coefficient α of 0.7. The coverage weight β is 0.5. Finally, for our Laplacian Mixed Model, the rate-distortion trade-off hyperparameter λ from Eq. 10 is uniformly set to 0.0005 for all reported results

Comparison Experiments

We conducted extensive comparison experiments against state-of-the-art 3D reconstruction and rendering methods, including 3DGS (Kerbl et al. 2023), 2DGS (Huang et al. 2024), Scaffold-GS (Lu et al. 2024), Hierarchical-GS (Kerbl et al. 2024), Octree-GS (Ren et al. 2024), Context-GS (Wang et al. 2024) and HAC++ (Chen et al. 2025). Our evaluation focuses on key metrics such as rendering speed, memory usage, primitive number and reconstruction quality (PSNR, SSIM (Wang et al. 2004), LPIPS (Zhang et al. 2018)).

As demonstrated in Tab. 1, Tab. 2 and Fig. 3, our Pyramid-GS consistently achieves competitive rendering quality and efficiency across a diverse range of datasets. These datasets span a wide range of scales and complexities, from object-centric small scenes to large-scale autonomous driving and massive urban environments, allowing for a comprehensive evaluation of the capabilities of our method.

Specifically, Tab. 1 highlights the effectiveness of our Pyramid-GS on large-scale datasets. On Waymo dataset, our method achieved optimal rendering results with minimal memory consumption, underscoring the scalability and efficiency of our approach. For Matrix City, we achieved the best rendering quality, with memory consumption only slightly increasing compared to HAC++ and Context-GS. These results confirm the advantage of our hierarchical scene perception representation in significantly reducing the number of active Gaussians that need to be processed and stored, thereby improving memory efficiency on large scenes with the compression algorithm.

In contrast, Tab. 2 presents results for small-scale scenes, such as Mip-NeRF360 and Tanks & Temples. On Mip-NeRF360, our method achieved the most best results, while on Tanks & Temples, we reached a near-optimal state, notably utilizing the fewest Gaussians to achieve this rendering quality. This is because the Tanks & Temples are dense and involve more complex textures, while our model pays more attention to large-scale and efficient management than the rendering quality, so it can achieve suboptimal rendering quality with the least number of Gaussians. This reinforces our core contribution: a novel scene perception and compression framework for 3D Gaussian Splatting.

The experimental results reveal that our Pyramid-GS excels at maintaining high rendering quality across diverse scales due to our scene perception compensation algorithm. Furthermore, our pyramid representation and compression module fosters a flexible and memory-efficient scene representation. It allows for adaptive rendering that scales gracefully with scene complexity, preserving essential details even at lower levels of the hierarchy. We present qualitative results in Fig. 3, which show that our model maintains photorealistic rendering quality and handles complex geometry effectively across different scales. The performance gains are more significant in large-scale environments, confirming the robustness of our perceive-sample-compress approach.

Ablation Studies

To evaluate the contribution of each proposed component, we performed comprehensive ablation studies as shown in Tab. 3, and Fig. 4.

Impact of Scene Perception Compensation First, we evaluate the importance of the scene perception compensation algorithm. We compare the Pyramid-GS with a variant that uses a camera distance-based level partition and mask without considering the scene compensation. The results in Tab 3 show that the disabling of scene perception compensation leads to a degradation in rendering quality. In certain complex scenes, relying solely on distance can cause important details to be oversimplified. The depth and cov-

Table 1: Quantitative comparison on Waymo (Sun et al. 2020) and MatrixCity (Li et al. 2023) datasets. The color of each cell shows the **best** and the **second best**.

Dataset Method	Waymo (Sun et al. 2020)					MatrixCity (Li et al. 2023)				
	SSIM↑	PSNR↑	LPIPS↓	#GS(k)↓	Mem(MB)↓	SSIM↑	PSNR↑	LPIPS↓	#GS(k)↓	Mem(MB)↓
3DGS (Kerbl et al. 2023)	0.840	27.19	0.313	1530	382.6	0.823	26.82	0.246	1432	3387.4
2DGS (Huang et al. 2024)	0.801	24.83	0.373	860	187.1	0.818	26.28	0.232	832	1659.1
Hierarchical-GS (Kerbl et al. 2024)	0.808	24.85	0.307	530	1035.7	0.823	27.69	0.276	271	1866.7
Scaffold-GS (Lu et al. 2024)	0.843	27.51	0.310	175	104.2	0.868	29.00	0.210	357	371.2
Octree-GS (Ren et al. 2024)	0.828	26.82	0.321	171	97.5	0.887	29.83	0.192	360	380.3
ContextGS (Wang et al. 2024)	0.847	27.93	0.310	133	11.1	0.878	29.26	0.188	221	30.3
HAC++ (Chen et al. 2025)	0.846	27.68	0.311	124	15.7	0.884	29.29	0.175	206	39.5
Ours	0.851	28.18	0.300	105	9.5	0.896	30.08	0.154	406	44.0

Table 2: Quantitative comparison on Mip-NeRF360 (Barron et al. 2022) and Tanks & Temples (Knapitsch et al. 2017). The color of each cell shows the **best** and the **second best**.

Dataset Method	Mip-NeRF360 (Barron et al. 2022)					Tanks & Temples (Knapitsch et al. 2017)				
	SSIM↑	PSNR↑	LPIPS↓	#GS(k)↓	Mem(MB)↓	SSIM↑	PSNR↑	LPIPS↓	#GS(k)↓	Mem(MB)↓
3DGS (Kerbl et al. 2023)	0.870	28.69	0.182	962	754.7	0.844	23.69	0.178	765	430.1
2DGS (Huang et al. 2024)	0.863	28.53	0.201	399	390.4	0.830	23.25	0.212	352	204.4
Scaffold-GS (Lu et al. 2024)	0.870	29.35	0.188	658	182.6	0.853	23.96	0.177	626	167.5
Octree-GS (Ren et al. 2024)	0.867	29.11	0.188	695	140.4	0.866	24.68	0.153	443	88.5
ContextGS (Wang et al. 2024)	0.868	29.30	0.194	685	19.9	0.855	24.29	0.176	469	11.8
HAC++ (Chen et al. 2025)	0.865	29.26	0.207	680	16.0	0.854	24.32	0.178	481	8.6
Ours	0.876	29.39	0.187	377	15.8	0.847	24.32	0.174	317	11.7

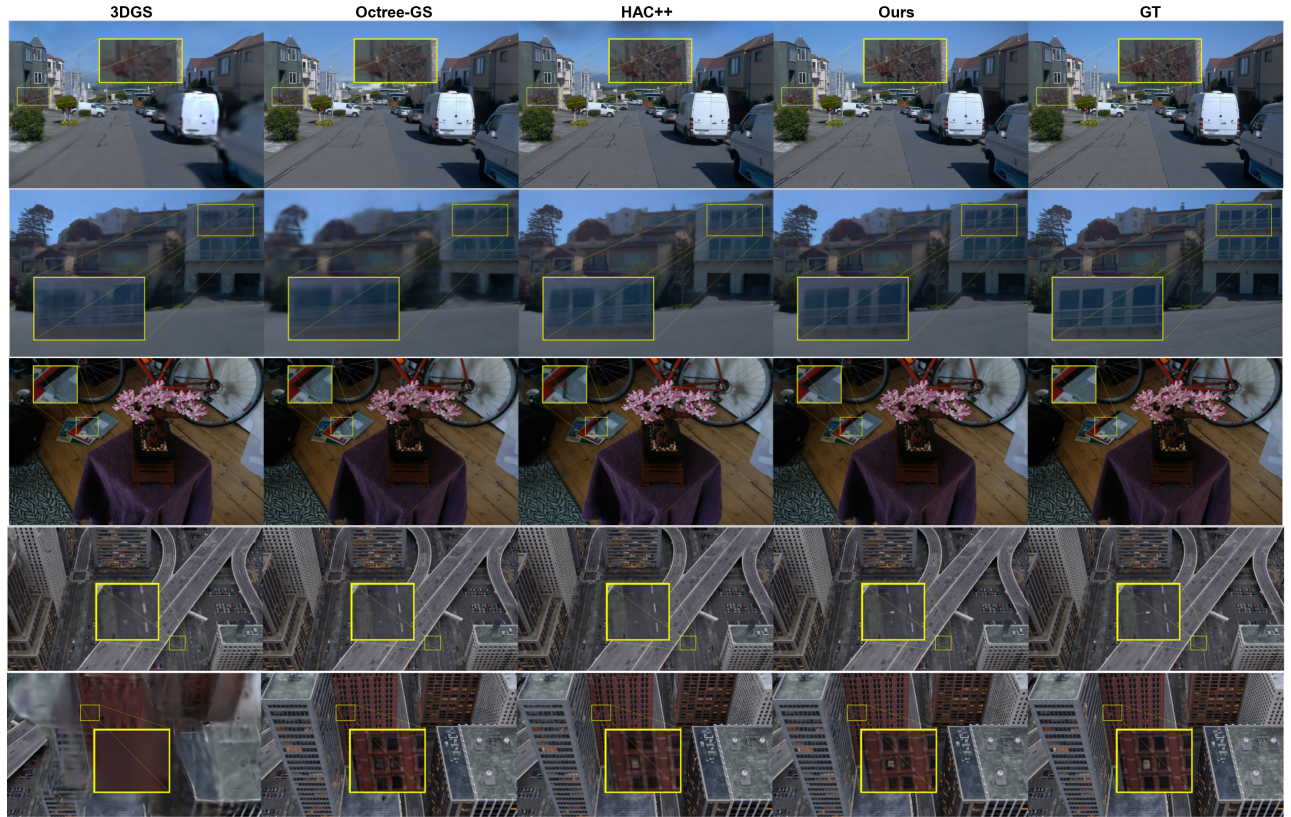


Figure 3: **Comparison Results.** Visual differences are highlighted with yellow insets for better clarity. Our approach consistently outperforms other models on different scenes, demonstrating advantages in challenging scenarios. Best viewed in color.



Figure 4: **Effect of Scene Perception Compensation.** While relying solely on camera distance can work well in most situations, in some extreme scenes it may fail and result in poor rendering results. This is because that too many key points are ignored by the algorithm. Through our algorithm, the model can correct errors and preserve details.

erage compensation ensures that Gaussians relevant to the viewer’s perspective are prioritized, leading to better perceptual quality and more efficient rendering of visually significant features. As shown in Fig. 4, in some extreme situations, the camera distance-based function will lose control and fail to optimize the scene reconstruction.

Table 3: Ablation study of different components on Waymo dataset, where SPC means the scene perception compensation algorithm, PS denotes pyramid sampling.

	SSIM \uparrow	PSNR \uparrow	LPIPS \downarrow	#GS(k) \downarrow	Mem(MB) \downarrow
w/o SPC	0.833	27.12	0.312	138	14.5
w/o PS	0.845	27.95	0.301	154	17.2
w/o SPC & PS	0.846	27.90	0.308	115	11.3
w/o Compression	0.847	27.96	0.301	144	81.3
Ours	0.851	28.18	0.300	105	9.5

Impact of Pyramid Sampling We evaluate the efficacy of our Laplacian pyramid-based hierarchical representation against a baseline approach that uses only voxelization without the multi-level aggregation. As shown in Table 3, the full Pyramid-GS with Laplacian pyramid representation significantly reduces the number of active Gaussians. This hierarchical structure not only decreases the number of primitive by about 30% compared to simple voxelization but also leads to a noticeable improvement in reconstruction quality. This highlights the benefit of our multi-level aggregation strategy for efficient scene management.

When we replace the pyramid representation with the Octree-GS, we can observe a degradation in rendering quality, this is because we can avoid over-pruning important points through a backward upsampling process.

Impact of Compression Algorithm Finally, we evaluate the effectiveness of our Generalized Gaussian Mixed

Table 4: Ablation study on density threshold λ on Waymo dataset. Increasing λ reduces memory consumption and number of Gaussian primitive, but slightly affects quality.

λ	SSIM \uparrow	PSNR \uparrow	LPIPS \downarrow	#GS(k) \downarrow	Mem(MB) \downarrow	FPS \uparrow
0.0005	0.851	28.18	0.300	105	9.5	138
0.0014	0.848	28.07	0.310	81	6.9	152
0.0018	0.846	27.95	0.315	76	6.0	159
0.0030	0.842	27.80	0.322	66	5.1	161
0.0040	0.839	27.65	0.329	56	4.1	163

compression algorithm for storing the Gaussian representations. Tab. 3 demonstrates that our compression algorithm can achieve significant size reductions with minimal impact on rendering quality. When replacing it with the Gaussian Mixed model used in HAC++, we can observe a degradation in both rendering quality and memory consumption. This highlights the efficiency of our compression scheme, which leverages the structure of the pyramid to effectively represent Gaussian primitives with fewer parameters, making our Pyramid-GS highly practical for storage and deployment.

Table 5: Comparison of training, encoding, and decoding time across different methods.

Method	Training Time	Enc. Time(s)	Dec. Time(s)
Octree-GS (Ren et al. 2024)	49min	-	-
Context-GS (Wang et al. 2024)	1h58min	78.39	72.59
HAC++ (Chen et al. 2025)	1h34min	30.81	48.81
Ours	1h38min	16.31	28.95

Discussion

We explore the relationship between the compression rate, rendering quality, speed, and final storage size by adjusting the λ . Tab. 4 shows that increasing λ results in higher compression rates, which reduces the final storage size and increase the FPS. However, this also leads to a decrease in rendering quality. These findings highlight the trade-offs involved: higher compression leads to more compact storage and faster rendering but at the expense of visual fidelity.

Additionally, we observe that our method has comparable enc/dec times for compression and overall training times to HAC++, indicating similar computational efficiency in Tab. 5. This demonstrates that our approach maintains competitive performance while achieving effective compression. As for the training time, it is longer than non-compression methods. This is because joint optimization takes more time.

Conclusion

In this paper, we proposed Pyramid-GS, a novel approach to 3D Gaussian Splatting that leverages a hierarchical scene perception and compression representation for efficient primitive management. Through extensive experiments across diverse datasets, we demonstrated the effectiveness and scalability of our method in both small-scale and large-scale environments. Our ablation studies further validated the contributions of key components, emphasizing the importance of scene perception compensation, pyramid sam-

pling and compression algorithm. The results indicate that Pyramid-GS not only enhances rendering quality but also significantly improves computational efficiency, making it a valuable tool for various applications in 3D reconstruction.

References

- Ali, M. S.; Qamar, M.; Bae, S.-H.; and Tartaglione, E. 2024. Trimming the fat: Efficient compression of 3d gaussian splats through pruning. *arXiv preprint arXiv:2406.18214*.
- Avidan, S.; and Shashua, A. 1997. Novel view synthesis in tensor space. In *Proceedings of IEEE computer society conference on computer vision and pattern recognition*, 1034–1040. IEEE.
- Barron, J. T.; Mildenhall, B.; Verbin, D.; Srinivasan, P. P.; and Hedman, P. 2022. Mip-nerf 360: Unbounded anti-aliased neural radiance fields. In *Proceedings of the IEEE/CVF conference on computer vision and pattern recognition*, 5470–5479.
- Chen, J.; Ye, W.; Wang, Y.; Chen, D.; Huang, D.; Ouyang, W.; Zhang, G.; Qiao, Y.; and He, T. 2024a. Gigags: Scaling up planar-based 3d gaussians for large scene surface reconstruction. *arXiv preprint arXiv:2409.06685*.
- Chen, Y.; Wu, Q.; Lin, W.; Harandi, M.; and Cai, J. 2024b. Hac: Hash-grid assisted context for 3d gaussian splatting compression. In *European Conference on Computer Vision*, 422–438. Springer.
- Chen, Y.; Wu, Q.; Lin, W.; Harandi, M.; and Cai, J. 2025. Hac++: Towards 100x compression of 3d gaussian splatting. *arXiv preprint arXiv:2501.12255*.
- Choi, I.; Gallo, O.; Troccoli, A.; Kim, M. H.; and Kautz, J. 2019. Extreme view synthesis. In *Proceedings of the IEEE/CVF international conference on computer vision*, 7781–7790.
- Cui, J.; Cao, J.; Zhao, F.; He, Z.; Chen, Y.; Zhong, Y.; Xu, L.; Shi, Y.; Zhang, Y.; and Yu, J. 2024. Letsgo: Large-scale garage modeling and rendering via lidar-assisted gaussian primitives. *ACM Transactions on Graphics (TOG)*, 43(6): 1–18.
- Dalal, A.; Hagen, D.; Robbersmyr, K. G.; and Knausgård, K. M. 2024. Gaussian splatting: 3D reconstruction and novel view synthesis: A review. *IEEE Access*, 12: 96797–96820.
- David, L.; Reddy, M.; Cohen, J.; Varshney, A.; Watson, B.; and Huebner, R. 2003. Level of detail for 3D graphics.
- Fan, Z.; Wang, K.; Wen, K.; Zhu, Z.; Xu, D.; Wang, Z.; et al. 2024. Lightgaussian: Unbounded 3d gaussian compression with 15x reduction and 200+ fps. *Advances in neural information processing systems*, 37: 140138–140158.
- Girish, S.; Gupta, K.; and Shrivastava, A. 2024. Eagles: Efficient accelerated 3d gaussians with lightweight encodings. In *European Conference on Computer Vision*, 54–71. Springer.
- Huang, B.; Yu, Z.; Chen, A.; Geiger, A.; and Gao, S. 2024. 2d gaussian splatting for geometrically accurate radiance fields. In *ACM SIGGRAPH 2024 conference papers*, 1–11.
- Kerbl, B.; Kopanas, G.; Leimkühler, T.; and Drettakis, G. 2023. 3D Gaussian splatting for real-time radiance field rendering. *ACM Trans. Graph.*, 42(4): 139–1.
- Kerbl, B.; Meuleman, A.; Kopanas, G.; Wimmer, M.; Lanvin, A.; and Drettakis, G. 2024. A hierarchical 3d gaussian representation for real-time rendering of very large datasets. *ACM Transactions on Graphics (TOG)*, 43(4): 1–15.
- Knapitsch, A.; Park, J.; Zhou, Q.-Y.; and Koltun, V. 2017. Tanks and temples: Benchmarking large-scale scene reconstruction. *ACM Transactions on Graphics (ToG)*, 36(4): 1–13.
- Lee, J. C.; Rho, D.; Sun, X.; Ko, J. H.; and Park, E. 2024. Compact 3d gaussian representation for radiance field. In *Proceedings of the IEEE/CVF Conference on Computer Vision and Pattern Recognition*, 21719–21728.
- Li, Y.; Jiang, L.; Xu, L.; Xiangli, Y.; Wang, Z.; Lin, D.; and Dai, B. 2023. Matrixcity: A large-scale city dataset for city-scale neural rendering and beyond. In *Proceedings of the IEEE/CVF International Conference on Computer Vision*, 3205–3215.
- Liu, X.; Wu, X.; Zhang, P.; Wang, S.; Li, Z.; and Kwong, S. 2024a. Compgs: Efficient 3d scene representation via compressed gaussian splatting. In *Proceedings of the 32nd ACM International Conference on Multimedia*, 2936–2944.
- Liu, Y.; Luo, C.; Fan, L.; Wang, N.; Peng, J.; and Zhang, Z. 2024b. Citygaussian: Real-time high-quality large-scale scene rendering with gaussians. In *European Conference on Computer Vision*, 265–282. Springer.
- Lombardi, S.; Simon, T.; Saragih, J.; Schwartz, G.; Lehrmann, A.; and Sheikh, Y. 2019. Neural volumes: Learning dynamic renderable volumes from images. *arXiv preprint arXiv:1906.07751*.
- Lu, T.; Yu, M.; Xu, L.; Xiangli, Y.; Wang, L.; Lin, D.; and Dai, B. 2024. Scaffold-gs: Structured 3d gaussians for view-adaptive rendering. In *Proceedings of the IEEE/CVF Conference on Computer Vision and Pattern Recognition*, 20654–20664.
- Milef, N.; Seyb, D.; Keeler, T.; Nguyen-Phuoc, T.; Božič, A.; Kondguli, S.; and Marshall, C. 2025. Learning fast 3D gaussian splatting rendering using continuous level of detail. In *Computer Graphics Forum*, e70069. Wiley Online Library.
- Navaneet, K.; Meibodi, K. P.; Koohpayegani, S. A.; and Pirsivavash, H. 2023. Compact3d: Compressing gaussian splat radiance field models with vector quantization. *arXiv preprint arXiv:2311.18159*, 2(3).
- Niedermayr, S.; Stumpfegger, J.; and Westermann, R. 2024. Compressed 3d gaussian splatting for accelerated novel view synthesis. In *Proceedings of the IEEE/CVF Conference on Computer Vision and Pattern Recognition*, 10349–10358.
- Papantonakis, P.; Kopanas, G.; Kerbl, B.; Lanvin, A.; and Drettakis, G. 2024. Reducing the memory footprint of 3d gaussian splatting. *Proceedings of the ACM on Computer Graphics and Interactive Techniques*, 7(1): 1–17.
- Penner, E.; and Zhang, L. 2017. Soft 3d reconstruction for view synthesis. *ACM Transactions on Graphics (TOG)*, 36(6): 1–11.

Ren, K.; Jiang, L.; Lu, T.; Yu, M.; Xu, L.; Ni, Z.; and Dai, B. 2024. Octree-gs: Towards consistent real-time rendering with lod-structured 3d gaussians. *arXiv preprint arXiv:2403.17898*.

Riegler, G.; and Koltun, V. 2020. Free view synthesis. In *European conference on computer vision*, 623–640. Springer.

Seo, Y.; Choi, Y. S.; Son, H. S.; and Uh, Y. 2024. Flod: Integrating flexible level of detail into 3d gaussian splatting for customizable rendering. *arXiv preprint arXiv:2408.12894*.

Sun, P.; Kretschmar, H.; Dotiwalla, X.; Chouard, A.; Patnaik, V.; Tsui, P.; Guo, J.; Zhou, Y.; Chai, Y.; Caine, B.; et al. 2020. Scalability in perception for autonomous driving: Waymo open dataset. In *Proceedings of the IEEE/CVF conference on computer vision and pattern recognition*, 2446–2454.

Wang, Y.; Li, Z.; Guo, L.; Yang, W.; Kot, A.; and Wen, B. 2024. Contextgs: Compact 3d gaussian splatting with anchor level context model. *Advances in neural information processing systems*, 37: 51532–51551.

Wang, Z.; Bovik, A. C.; Sheikh, H. R.; and Simoncelli, E. P. 2004. Image quality assessment: from error visibility to structural similarity. *IEEE transactions on image processing*, 13(4): 600–612.

Wang, Z.; and Xu, D. 2024. Pygs: Large-scale scene representation with pyramidal 3d gaussian splatting. *arXiv preprint arXiv:2405.16829*.

Watson, D.; Chan, W.; Martin-Brualla, R.; Ho, J.; Tagliasacchi, A.; and Norouzi, M. 2022. Novel view synthesis with diffusion models. *arXiv preprint arXiv:2210.04628*.

Wizadwongsa, S.; Phongthawee, P.; Yenphraphai, J.; and Suwajanakorn, S. 2021. Nex: Real-time view synthesis with neural basis expansion. In *Proceedings of the IEEE/CVF Conference on Computer Vision and Pattern Recognition*, 8534–8543.

Yariv, L.; Hedman, P.; Reiser, C.; Verbin, D.; Srinivasan, P. P.; Szeliski, R.; Barron, J. T.; and Mildenhall, B. 2023. Baked sdf: Meshing neural sdfs for real-time view synthesis. In *ACM SIGGRAPH 2023 conference proceedings*, 1–9.

Zhang, R.; Isola, P.; Efros, A. A.; Shechtman, E.; and Wang, O. 2018. The unreasonable effectiveness of deep features as a perceptual metric. In *Proceedings of the IEEE conference on computer vision and pattern recognition*, 586–595.

Zhou, T.; Tucker, R.; Flynn, J.; Fyffe, G.; and Snavely, N. 2018. Stereo magnification: Learning view synthesis using multiplane images. *arXiv preprint arXiv:1805.09817*.